Int. J. Multiphase Flow Vol. 16, No. 5, pp. 799–817, 1990
Printed in Great Britain.

0301-9322/90 $3.00 + 0.00

TWO-PHASE FLOW THROUGH PIPE BRANCH JUNCTIONS

M. R. DAVIS[1] and B. FUNGTAMASAN[2]

[1]Department of Civil and Mechanical Engineering, University of Tasmania, G.P.O. Box 252C, Hobart, Tasmania 7001, Australia

[2]King Mongkut's Institute of Technology, Bangkok, Thailand

(*Received* 10 *September* 1988; *in revised form* 11 *January* 1990)

Abstract—Detailed distributions of void fraction and velocity are observed for flow in the vicinity of a junction where a side branch draws a flow from a vertical main pipe flow of a gas–liquid mixture in the froth–bubbly flow regime. Velocity ratio, momentum and energy distribution parameters determined from these needle void probe measurements are then combined with the equations for compressible mixture flow to facilitate the determination of the branch junction force and pressure loss coefficients. Values of these coefficients were found to be of comparable magnitude to those found in single-phase flow through a junction, although some significant variations due to the larger proportion of the gas phase diverted to the branch were observed. This larger proportion of gas phase division to the branch increased with the mixture void fraction and overall branch flow rate. Whilst the branch flow was stratified, it was found to be significantly less intermittent in nature than the main inlet and outlet flows. Pulsations in the void fraction were between 0.2 of the local mean void fraction in the branch and 0.6 in the main outlet flow, which also tended to exhibit a characteristic frequency of voidage pulsation.

Key Words: two-phase flow, gas–liquid flow, pipe junctions

1. INTRODUCTION

Fluid flow into a side branch from a pipe flow depends upon the inter-relation between flow rates to the branch and main pipes downstream of the junction and the pressure loss between the single main inlet flow and the two outlet flows. For single-phase flows this problem has been modelled in terms of a momentum balance at the junction by Vogel (1926/28), Enger & Levy (1929) and Acrivos (1959), who introduced empirical relations between the net forces on the solid walls of the junction and the momentum fluxes of the flows. These forces depend, of course, upon the pressure distributions in the immediate vicinity of the junction and could only be determined on an empirical basis. This approach was extended by Benson & Woolatt (1966) for compressible single-phase flow and to include both momentum equations in the direction of the main flow and in the direction along the branch pipe, finding that the pressure drop to the main and side branches could be represented by

$$p_2 - p_1 = k_1(\rho_1 u_1^2 - \rho_2 u_2^2) \qquad [1]$$

and

$$p_1 - p_3 = k_2(\rho_3 u_3^2), \qquad [2]$$

where suffices 1, 2 and 3 denote inlet, main outlet and branch outlet, respectively. Whilst such a simplified representation of pressure drop may only be valid under certain restricted conditions, it is clear that [1] and [2] are an oversimplification, in general, and might not be particularly accurate under all possible conditions of flow. However, they illustrate the general approach to normalization of junction pressure drops which is adopted, with variations in detail, to correlate data under varying conditions of junction geometry and flow. The flow density, velocity and pressure are denoted by ρ, u and p, respectively, and it was found that $k_1 \simeq 0.7$, and that k_2 was in the range 0.3–0.6. Subsequently, a number of more detailed investigations of single-phase junction flows were carried out by McNown (1954), Zeisser (1963) and Bajura (1971), whilst Jamison & Villemonte (1971), Miller (1978) and Williamson & Rhone (1973) investigated the flows in terms of the energy loss between the inlet and two outlet flows. The majority of investigations have dealt with a perpendicular branch with a dividing (as opposed to joining) flow direction. Ito & Imai (1973) and

others have considered the influence of the sharpness of the junction edges, whilst a dominant parameter in many investigations has been the ratio of branch to main pipe diameters.

Under two-phase flow conditions the behaviour of the branch junction is complicated considerably by the structure of the gas–liquid mixture and, in particular, by its influence on the relative division of the two phases to the main and branch outlets, which becomes a parameter of great significance in the overall design of two-phase flow systems (Tsuyama & Taga 1959). Various attempts have been made to establish a basis for manifold designs providing equal quality for vapour–liquid mixtures to all outlets (Greene 1967; Fouda & Rhodes 1972, 1974), whilst Oranje (1973) has considered the occurrence of favoured routes for the liquid phase in complex natural gas flow systems. This work and that of Hong (1978) have primarily been concerned with quite high quality flows. Azzopardi & Whalley (1982) investigated the subdivision of two-phase flow at a junction, paying particular attention to the concept of extraction from a segment of the main pipe flow under annular flow conditions. Investigations at lower mixture qualities have been carried out by Collier (1976) and Honan & Lahey (1978). These showed a strong tendency for the gas phase to pass to the branch rather than to the main outlet pipe, and diagrams showing the proportionate division of phases passing to the two outlet flows were shown to demonstrate this to increase with inlet quality or void fraction. Pressure drop data were considered in a manner somewhat similar to that established for single-phase flow by Madden & St Pierre (1970), Fouda & Rhodes (1974) and Tsuyama & Taga (1959).

The purpose of the present paper is to carry out a much more detailed investigation of the two-phase flow structure in the vicinity of the junction using the void probe technique developed by Herringe & Davis (1974, 1976) to investigate velocity, void fraction and bubble size distributions within the flow. In addition, the techniques developed by Fungtamasan & Davis (1984) also provide an experimental insight into the occurrence and propagation of intermittent structures within froth or bubbly flows (i.e. as distinct from slug flows where this intermittency develops to its logical limit). This more detailed investigation also makes possible the inclusion of velocity ratio or relative motion effects determined from the flow structure measurements in the consideration of pressure losses.

2. ANALYSIS OF TWO-PHASE FLOW THROUGH A BRANCH JUNCTION

Gas–liquid mixtures have inertia, which is dominated by the liquid phase, and compressibility, which is dominated by the gas phase. In addition, the average velocity of the two phases is not necessarily the same. Thus, in considering the behaviour of gas–liquid mixture flows and in comparing this with that of single-phase flows, it is necessary to take account of these effects in terms of the compressible nature of the flow and the velocity ratio (S, the ratio of cross-sectional average gas velocity $\langle u_G \rangle$ to that of the liquid $\langle u_L \rangle$, where $\langle\ \rangle$ denotes the area average over the cross-section). For gas–liquid mixture flows the absence of transfer between the phases makes it possible to relate the local average mixture density ρ_m to a reference inlet condition, denoted by suffix 1, where

$$\rho_m = \epsilon \rho_{G1} \bar{p} + (1 - \epsilon)\rho_L, \qquad [3]$$

where $\bar{p}$ = dimensionless pressure = p/p_1, ϵ is the void fraction and ρ is the density of the mixture, gas or liquid according to the suffix. (In this and subsequent equations where area averages are implied, the notation $\langle\ \rangle$ is omitted for brevity, except in a few cases where it is needed to emphasize the methods of area averaging.) With no transfer between phases, the void fraction is then given by the following equation if isothermal compression of the gas phase is assumed:

$$\frac{\epsilon}{\epsilon_1} = \left[\left(\frac{S}{S_1}\right)(1 - \epsilon_1) + \epsilon_1 \bar{p}^{-1}\right] \bar{p}^{-1}. \qquad [4]$$

If we introduce the fraction σ of the inlet mass flow which is diverted to the branch, then the conservation equations of mass flow of each phase can be combined with the above equations

applied between inlet, branch outlet (suffix 3) and main outlet (suffix 2) to give the following expressions for void fraction in terms of the outlet pressures:

$$\left(\frac{\epsilon_3}{\epsilon_1}\right) = \left\{\left[\left(\frac{\sigma_L}{\sigma_G}\right)\left(\frac{S_3}{S_1}\right)(1-\epsilon_1) + \epsilon_1 \bar{p}_3^{-1}\right]\bar{p}_3\right\}^{-1} \quad [5]$$

and

$$\left(\frac{\epsilon_2}{\epsilon_1}\right) = \left\{\left[\frac{(1-\sigma_L)}{(1-\sigma_G)}\left(\frac{S_2}{S_1}\right)(1-\epsilon_1) + \epsilon_1 \bar{p}_2^{-1}\right]\bar{p}_2\right\}^{-1}. \quad [6]$$

Expressions for the density of branch and main outlet flows then follow directly from [3].

The flow through the junction can be analysed on a momentum basis if the net boundary forces due to normal pressure on the pipe walls are introduced as F_x in the main outlet direction and F_y in the branch direction (figure 1). If we follow the approach of Katz (1967) and Bajura (1971) for single-phase flow, then these forces are related by coefficients, k_x and k_y, to the inlet flow mass flux density and the branch flow velocity as follows:

$$F_x = k_x\{\rho_{G1}\langle\epsilon_1 u_{G1}\rangle\langle u_{G3}\rangle + \rho_L\langle(1-\epsilon_1)u_{L1}\rangle\langle u_{L3}\rangle\}A_3 \quad [7]$$

and

$$F_y = k_y\left(\frac{F_x}{k_x}\right). \quad [8]$$

Alternative definitions of coefficients describing these out of balance forces on the junction are of course possible, but in general it is possible to relate such alternative coefficients to those defined here and the approach of Katz (1967) is adopted for the purposes of comparison with single-phase flow. It then follows that the pressures in the main and branch outlets can be related to the inlet flow conditions and the coefficients k_x and k_y by writing momentum balance equations in the two

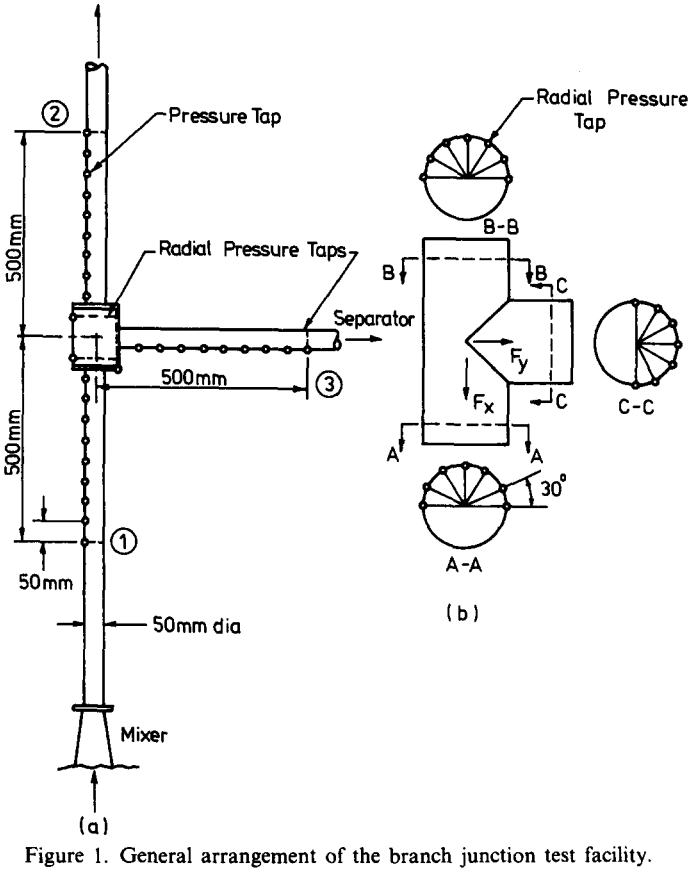

Figure 1. General arrangement of the branch junction test facility.

directions. The main outlet and branch pressures (p_2 and p_3) introduced represent the pressures corresponding to the extrapolation to the junction of the frictional pressure drop lines which are established in the outlet flows once the flows have established frictional pipe flow conditions. Accordingly, frictional effects on the walls are not included directly and the effect of the junction is expressed completely in terms of the net forces F_x and F_y. The resulting equations for the pressure change across the junction are then

$$\frac{p_1 - p_2}{p_1} = 1 - \bar{p}_2 = D_1 \left\{ \frac{(\rho_G \epsilon u_G^2 + \rho_L (1-\epsilon) u_L^2)_2}{(\rho_G \epsilon u_G^2 + \rho_L (1-\epsilon) u_L^2)_1} + \frac{k_x \left[\rho_{G1} \epsilon_1 u_{G1} u_{G3} + \rho_L (1-\epsilon_1) u_{L3} \left(\frac{A_3}{A_1} \right) \right]}{(\rho_G \epsilon u_G^2 + \rho_L (1-\epsilon) u_L^2)_1} - 1 \right\} \quad [9]$$

and

$$\frac{p_1 - p_3}{p_1} = 1 - \bar{p}_3 = D_1 \left\{ \frac{(\rho_G \epsilon u_G^2 + \rho_L (1-\epsilon) u_L^2)_3}{(\rho_G \epsilon u_G^2 + \rho_L (1-\epsilon) u_L^2)_1} - \frac{k_y [\rho_{G1} \epsilon_1 u_{G1} u_{G3} + \rho_L (1-\epsilon_1) u_{L1} u_{L3}]}{(\rho_G \epsilon u_G^2 + \rho_L (1-\epsilon) u_L^2)_1} \right\}, \quad [10]$$

where the parameter D represents the ratio of the mixture inertia to local pressure,

$$D = \frac{[\rho_G \epsilon u_G^2 + \rho_L (1-\epsilon) u_L^2]}{p}. \quad [11]$$

Note that the averaging symbols over the cross-section $\langle\ \rangle$ have been omitted to simplify the presentation, and that all quantities in [9] and [10] are area averaged. Upon substitution of the velocity ratio S and branch take-off fractions σ_L and σ_G, these equations can finally be rearranged as quadratic equations for the pressure changes across the junction:

$$\bar{p}_2^2 + \left[D_1 \left\{ \lambda_1 (1-\epsilon_1) + k_x \lambda_2 \left[(1-\epsilon_1) + \left(\frac{\sigma_G}{\sigma_L} \right) \left(\frac{S_1}{S_3} \right) \epsilon_1 \bar{p}_3^{-1} \right] - 1 \right\} - 1 \right] \bar{p}_2 + D_1 \lambda_1 \left[\frac{(1-\sigma_L)}{(1-\sigma_G)} \right] \left(\frac{S_1}{S_2} \right) \epsilon_1 = 0 \quad [12]$$

and

$$\bar{p}_3^2 + \left\{ D_1 \left[\lambda_3 \left(\frac{A_1}{A_3} \right)^2 - k_y \lambda_2 \left(\frac{A_1}{A_3} \right) \right] (1-\epsilon_1) - 1 \right\} \bar{p}_3 + D_1 \left\{ \lambda_3 \left(\frac{A_1}{A_3} \right)^2 - k_y \lambda_2 \left(\frac{A_1}{A_3} \right) \left(\frac{\sigma_G}{\sigma_L} \right) \left(\frac{S_1}{S_3} \right) \right\} \epsilon_1 = 0, \quad [13]$$

where

$$\lambda_1 = \left[\frac{(1-\sigma_G) \rho_{G1} \lambda_1 S_1 S_2 C_{G2} + (1-\sigma_L) \rho_L (1-\epsilon_1) C_{L2}}{\rho_{G1} \epsilon_1 S_1 C_{G1} + \rho_L (1-\epsilon_1) C_{L1}} \right] (1-\sigma_L), \quad [14]$$

$$\lambda_2 = \left[\frac{\rho_{G1} \epsilon_1 S_1 S_3 + \rho_L (1-\epsilon_1)}{\rho_{G1} \epsilon_1 S_1 C_{G1} + \rho_L (1-\epsilon_1) C_{L1}} \right] \sigma_L \quad [15]$$

and

$$\lambda_3 = \left[\frac{\sigma_G \rho_{G1} \epsilon_1 S_1 S_3 C_{G3} + \sigma_L \rho_L (1-\epsilon_1) C_{L3}}{\rho_{G1} \epsilon_1 S_1 C_{G1} + \rho_L (1-\epsilon_1) C_{L1}} \right] \sigma_L. \quad [16]$$

The coefficient C represents momentum distribution factors (see Yadigaroglu & Lahey 1976), given by

$$C_G = \frac{\langle \epsilon u_G^2 \rangle}{\langle \epsilon \rangle \langle u_G \rangle^2} \quad [17]$$

and

$$C_L = \frac{\langle (1-\epsilon) u_L^2 \rangle}{\langle 1-\epsilon \rangle \langle u_L \rangle^2}. \quad [18]$$

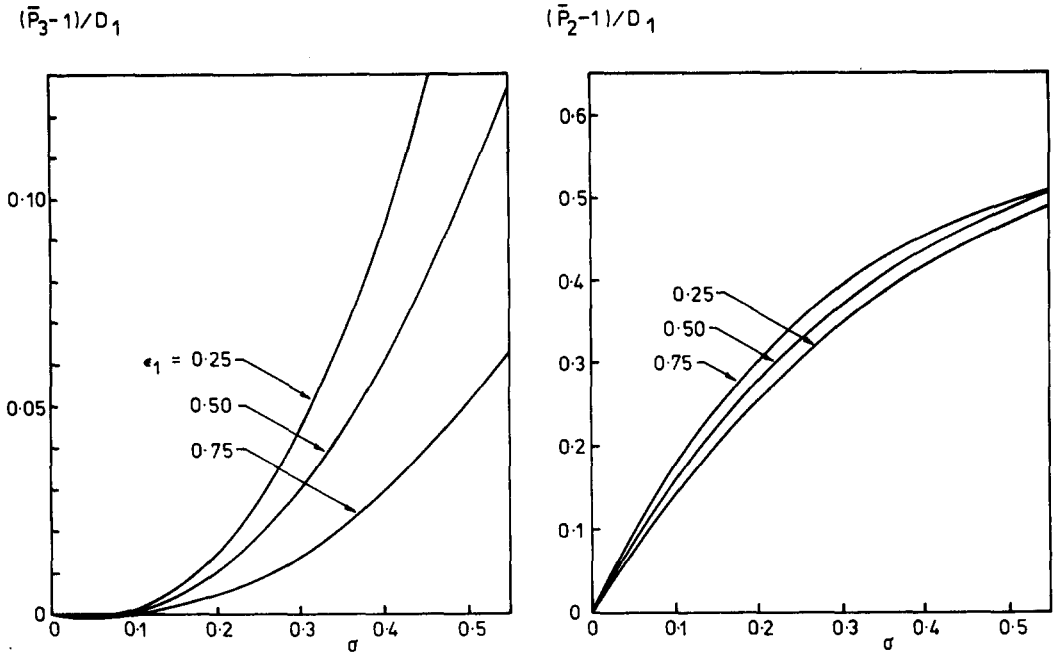

Figure 2. Variation of pressure changes across the junction (for homogeneous flow with $S = 1$, $D_1 = 0.5$, $k_x = 0.6$, $k_y = 0.1$).

We see from [12] and [13] that if the flow structural parameters (velocity ratio, void fraction, momentum distribution factors and flow subdivision fractions) are known from detailed internal observations of the flow, then it is possible to determine the coefficients k_x and k_y from the observed pressure changes $\bar{p}_2$ and $\bar{p}_3$. In the experimental work to be described in section 3, experimental observations of pressures are used as the basis for calculating k_x and k_y. It is clearly not possible to attempt to calculate the pressures in the flow without any basis for assuming particular values of k_x and k_y, and it is not the intention of the present work to presume any specific values of k_x and k_y in order to predict experimental flow pressures. Moreover, strong three-dimensional effects near the junction preclude consideration of the sections very near the junction in terms of a one-dimensional simplification.

In order to demonstrate the general trends for junction pressure changes, figure 2 illustrates pressures on the basis of presumed values of k_x and k_y. If the flows were homogenous (C_L, $C_G = 1$) and the velocity ratio was unity ($S = 1$), then the equations above simplify to a dependence of $\bar{p}_3$ and $\bar{p}_2$ upon the inlet flow parameters (D_1 and ϵ_1), the mixture subdivision fraction ($\sigma = \sigma_L = \sigma_G$) and the branch area ratio (A_3/A_1). Thus, p_3 is given by

$$\bar{p}_3 = \left\{ D_1 \sigma \left(\frac{A_1}{A_3} \right) \left[\sigma \left(\frac{A_1}{A_3} \right) - k_y \right] (1 - \epsilon_1) - 1 \right\}^{-1}; \qquad [19]$$

and $\bar{p}_2$ is given by solution of the quadratic equation

$$\bar{p}_2^2 + [\![D_1 \{ (1-\sigma)^2 (1-\epsilon_1) + k_x [\sigma(1-\epsilon_1) + \sigma\epsilon_1 \bar{p}_3^{-1}] - 1 \} - 1]\!] \bar{p}_2 + D_1 (1-\sigma)^2 \epsilon_1 = 0. \qquad [20]$$

Solutions of these equations are shown in figure 2 and it can be seen that the normalized pressure rise in the branch increases as the mixture void fraction decreases, whilst the main line pressure rise decreases. These effects and the curved form of the functions of the branch take-off fraction (σ) are due to the compressible nature of the flow since the pressure rises are shown in a form that is normalized in terms of the parameter ($\rho_m u_1^2$), which is based on the mixture average density (ρ_m) which is itself influenced by the inlet void fraction. It can be seen that the influence of the mixture void fraction on the branch pressure rise is substantially stronger than on the main outlet pressure rise. Figure 2 emphasizes the necessity of using the foregoing compressible mixture flow equations in the analysis of observed experimental pressure rise data, as described in the following sections.

3. OBSERVATIONS OF FLOW STRUCTURE

(i) Distributions of voidage and velocity

A general arrangement of the experimental system is shown in figure 1. Flows of water and air from pumps and a compressor were metered using standard orifice meters and were then passed through regulating valves to a conical mixing chamber. This was of the design described by Herringe & Davis (1974) and produced a well-mixed upward froth flow at its outlet, the flows being injected through a set of nozzles located in the baseplate of the conical chamber. The nozzle outlet and main vertical upward flow pipe line were of dia 50 mm. The branch junction under test was located 1.2 m above the conical mixer outlet, and the main vertical pipe continued in a vertical direction for a further 3.74 m before being discharged downwards through a U-bend and control valve to the atmosphere. The junction piece was machined from Perspex and was in the form of the intersection of the main vertical tube by a horizontal side branch without any additional machining to streamline the edges of the junction, apart from removal of burrs and smoothing of the actual edge. Two junctions were used, having horizontal side branches of 50 and 25 mm dia, each being polished after machining to allow observation of the flow. The horizontal branch extended at constant diameter to a distance of 1.3 m from the junction before discharging into a large separating chamber with a top exit for the air flow and a bottom exit for the water flow, each flow being metered by an orifice plate so that the total mass flows of gas and liquid in all three pipes at the junction could be calculated.

Experiments were carried out for flows which appeared to be of the bubbly or froth type having void fractions between 0.25 and 0.9 and velocity between 2 and 9 m/s in the various sections of the system. This placed the flows in the vicinity of the transitional boundary between finely dispersed bubble and churn flow on the flow regime map of Taitel *et al.* (1980), this being consistent with the appearance of the flows. Visual inspection, flash photography and high-speed film of the flows indicated that intermittent effects were present in the form of general concentrations of bubble clouds moving somewhat faster than the average mixture velocity, as described by Fungtamasan & Davis (1984).

Detailed observations of the flow structure were made using the resistivity needle probe method developed by Herringe & Davis (1974). The probes were of the double-needle type, with a streamwise separation of the two side-by-side stainless steel needle tips of 5 mm. The needles were insulated by epoxy except for a small zone near the tip with a radius of 6 μm and an exposed length of about 50 mm. Each needle was operated as part of a separate a.c. bridge and generated a two-state signal, indicating the presence of gas or liquid at the tip after appropriate demodulation and gating. The local mixture void fraction was determined by probability analysis of the front needle signal which showed a step at a position corresponding to the fraction of time gas was present at the tip (taken as the definition of point local void fraction), whilst the mixture local velocity was determined by cross-correlation of the two needle signals. These analyses were carried out using a Hewlett Packard 3721A correlation/probability analyser, and formed the basis for observations of detailed local voidage and velocity profiles across the flow.

Figures 3 and 4 show representative voidage and velocity profiles for the inlet, main outlet and branch pipes, respectively. In general, the inlet flows were relatively well-mixed, having only a small and symmetric variation of velocity across the section but with a more substantial variation of mixture void fraction. The main outlet flows generally showed a nearly symmetrical distribution of void fraction, whilst the velocity profiles showed a significantly higher velocity on the side adjacent to and above the branch exit. Owing to its horizontal orientation the branch pipe contained a substantial concentration of the gas phase towards the top of the cross-section, whilst the velocity profiles in the branch were relatively uniform and symmetrical. However, at higher mixture average velocity it was found that the branch pipe velocity profile showed a maximum in the region of higher local void fraction, particularly for the smaller branch, as illustrated in figures 3(b) and 4(b). Integration of these profiles in the inlet and both outlets to obtain the total gas phase volumetric flux over the whole cross-section indicated results that were generally within 5%, on average, of the flow metered external to the rig, the probe traverses giving slightly lower flow rates, presumably due to the deflection of some smaller bubbles or else due to the combination of the observations over only a few diameters with significant asymmetry of flow. These results also allow

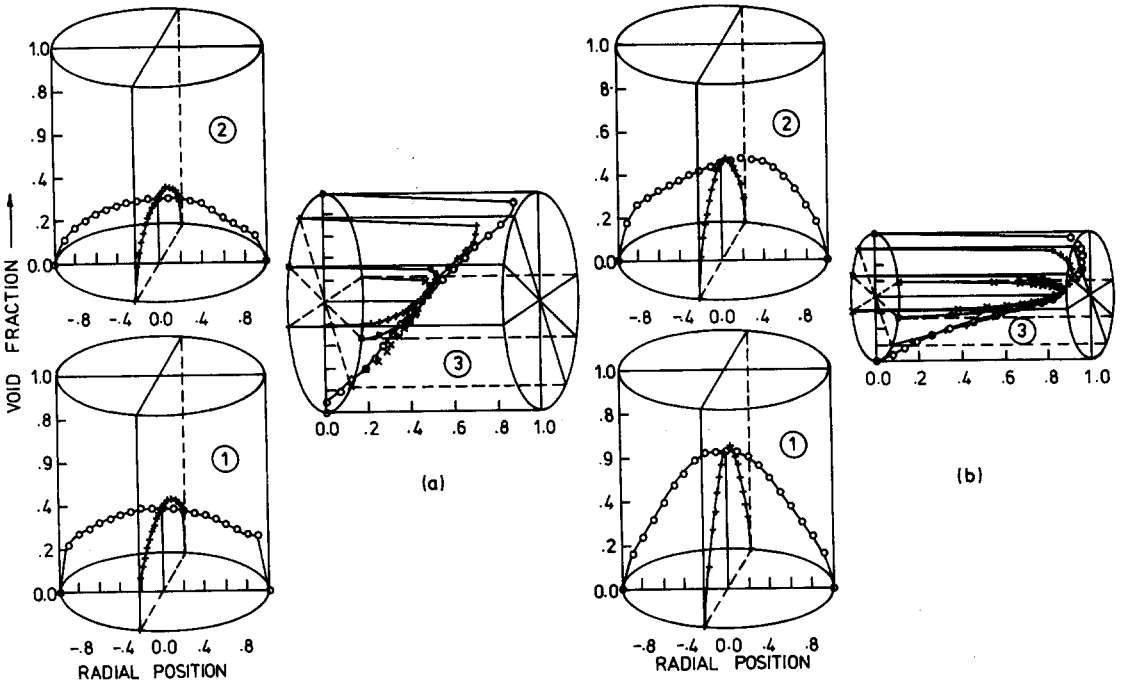

Figure 3. Voidage distributions in the vicinity of the junction. (a) $d_3/d_1 = 1.0$, flow condition 2; (b) $d_3/d_1 = 0.5$, flow condition 3.

determination of the average velocity ratios in terms of the area-averaged velocities (see Zuber & Findlay 1965) as

$$S = \frac{\langle u_G \rangle}{\langle u_L \rangle} = \frac{\langle \epsilon \rangle^{-1} - 1}{\beta^{-1} - 1}, \qquad [21]$$

where the angle brackets denote area average, ϵ is the total void fraction, β = gas volumetric flow/total volumetric flow and u_G and u_L are the gas and liquid velocities, respectively. Figure 5

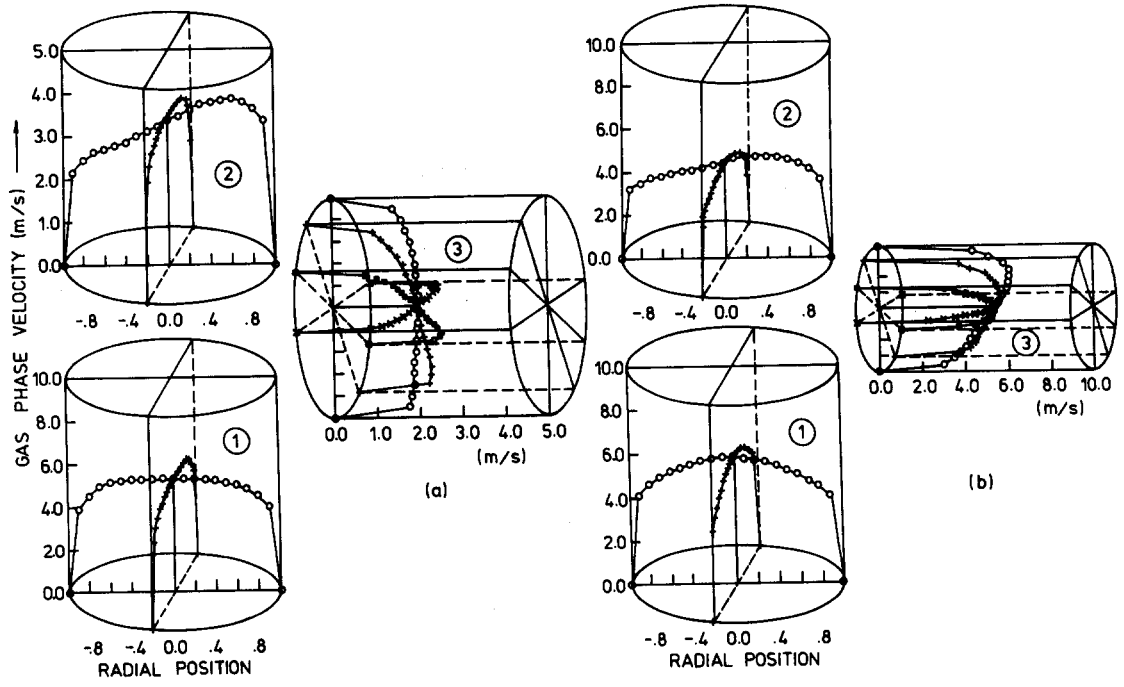

Figure 4. Velocity distributions in the vicinity of the junction. (a) $d_3/d_1 = 1.0$, flow condition 2; (b) $d_3/d_1 = 0.5$, flow condition 3.

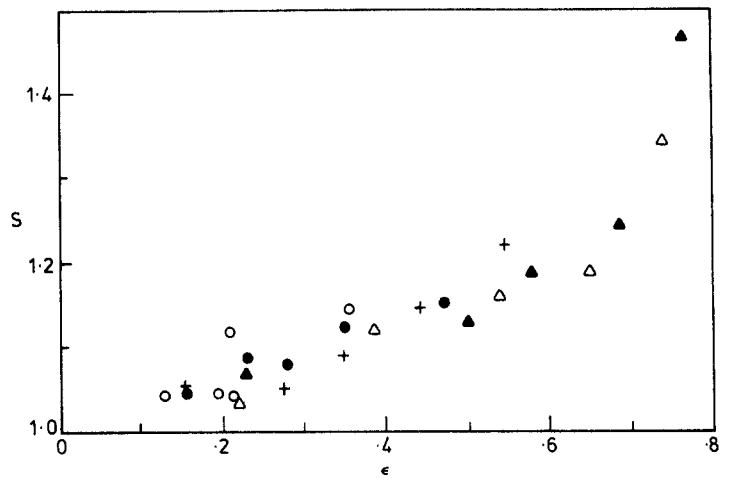

Figure 5. Velocity ratios observed in the vicinity of the junction (at sections 1, 2 and 3). +, Inlet; ○, main outlet ($d_3/d_1 = 1$); ●, main outlet ($d_3/d_1 = 0.5$); △, branch outlet ($d_3/d_1 = 1$); ▲, branch outlet ($d_3/d_1 = 0.5$).

shows that across all the observations there was a general tendency for the velocity ratio to increase with average void fraction, being in the range between 1.0 and 1.5.

The detailed profiles within the mixture flow observed with the void detection probes also allow determination of the gas phase momentum coefficient C_G, as defined in [17], which would be expected to have a similar value to C_L if the flows are locally well-mixed. Also, it is possible to determine kinetic energy correction factors C_{Ge} and C_{Le} for the gas and liquid phases, as defined by

$$C_{Ge} = \frac{\langle \epsilon u_G^3 \rangle}{\langle \epsilon \rangle \langle u_G \rangle^3} \qquad [22]$$

and

$$C_{Le} = \frac{\langle (1-\epsilon) u_L^3 \rangle}{\langle 1-\epsilon \rangle \langle u_L \rangle^3}. \qquad [23]$$

Values of the momentum and kinetic energy correction factors for the inlet and both outlet pipes are shown in table 1. Values in the inlet and main and branch outlets are shown for locations marked 1, 2 and 3 in figure 1. As voidage probe measurements were not taken at other positions along the pipes it is only possible to show detailed data at these particular sections. Moreover, strong three-dimensional effects very close to the junction preclude the use of the correction factors shown in table 1 in that region as they rely on the assumption that only the axial velocity components are significant. In general, these corrections for distribution effects lie between 1.0 and 28%, with the average of all values being about 5%. Since the flow structural data is available for all cases tested here, these correction factors are introduced in the calculations of the pressure loss and force coefficients in subsequent sections, together with the velocity ratios S measured in each case.

(ii) Distributions of bubble size and intermittent flow fluctuations

Bubble size distributions were measured using the techniques of Herringe & Davis (1976) by means of a pulse width to height converter, sample and hold system and probability analyser. Figure 6 shows the mean bubble size distributions of the inlet and outlet flows, indicated here as the mean of all detected streamwise chord sizes. A detailed discussion of alternative weightings in the calculation of bubble size (i.e. by detected chords, detected bubbles or by volumetric mean) is given by Herringe & Davis (1976). It can be seen that whilst the inlet flow has appreciably larger size bubbles at the centreline, with average detected chords of up to 10 mm, the bubble size reduces sharply (to around 2 mm for the larger side branch) and becomes more uniform in the main outlet pipe, in particular with the large branch where a larger branch flow is drawn off. In the lower half

Table 1. Flow conditions in the three pipe components and distribution factors observed by a void probe

Diameter ratio	Flow condition	Mass flow ratio		Inlet		Main outlet		Branch		Momentum distribution factor (C_G)			Kinetic energy distribution factor (C_{Ge})		
		σ_M ($\dot{m}_3/\dot{m}_1$)	σ_G (m_{G3}/m_{G1})	β	u_M (m/s)	β	u_M (m/s)	β	u_M (m/s)	Inlet	Main outlet	Branch	Inlet	Main outlet	Branch
1.0	1	0.44	0.78	0.47	2.92	0.27	1.10	0.62	1.81	1.020	1.026	1.012	1.050	1.071	1.031
	2	0.21	0.63	0.52	6.21	0.35	3.59	0.77	2.74	1.025	1.029	1.027	1.063	1.078	1.071
	3	0.21	0.54	0.56	5.57	0.30	3.41	0.78	2.27	1.021	1.024	1.027	1.056	1.063	1.056
	4	0.20	0.48	0.63	6.62	0.55	4.29	0.81	2.42	1.029	1.024	1.021	1.078	1.062	1.055
	5	0.33	0.80	0.69	4.96	0.42	1.81	0.85	3.45	1.045	1.027	1.038	1.128	1.072	1.105
	6	0.24	0.65	0.77	6.61	0.61	2.97	0.90	3.77	—	—	—	—	—	—
0.5	1	0.31	0.68	0.47	2.92	0.31	1.57	0.69	5.98	1.020	1.023	1.015	1.050	1.060	1.038
	2	0.12	0.53	0.51	6.20	0.49	5.17	0.73	4.95	1.025	1.032	1.023	1.063	1.089	1.060
	3	0.13	0.29	0.56	5.57	0.52	4.43	0.76	5.00	1.021	1.025	1.037	1.056	1.068	1.102
	4	0.14	0.40	0.65	6.62	0.55	4.67	0.84	8.46	1.029	1.024	1.037	1.078	1.064	1.145
	5	0.13	0.36	0.68	4.97	0.62	3.60	0.86	5.89	1.045	1.033	1.090	1.128	1.090	1.276
	6	0.13	0.48	0.76	6.60	0.67	4.04	0.93	11.1	—	—	—	—	—	—

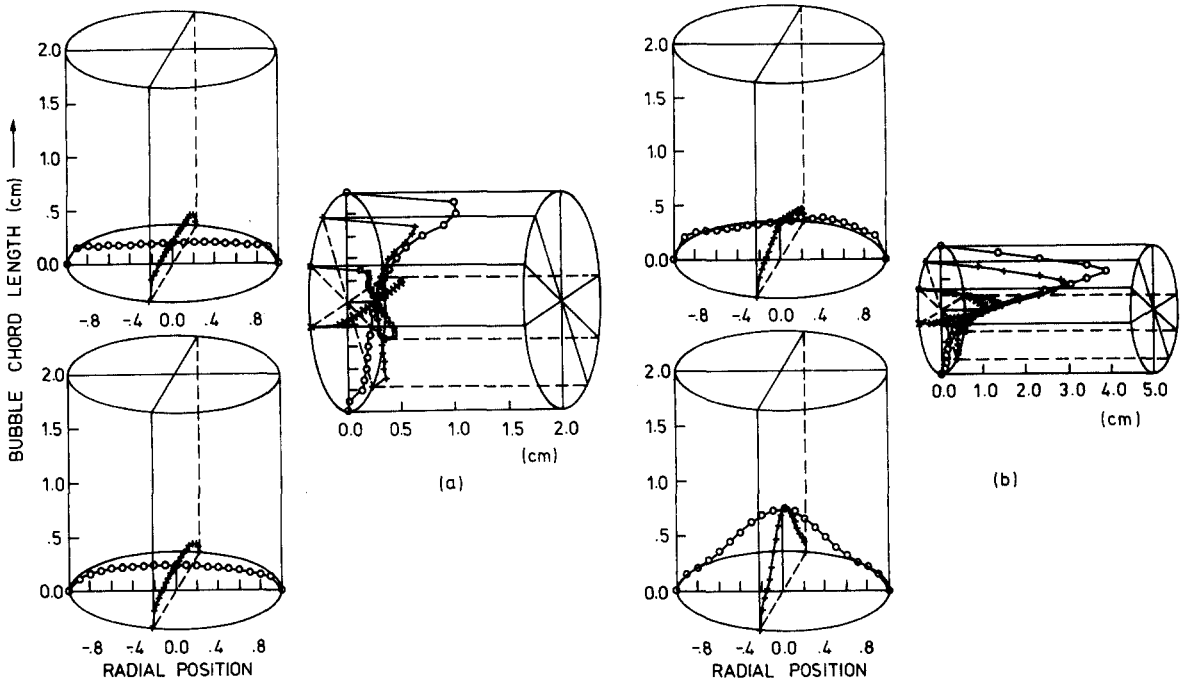

Figure 6. Mean bubble size distributions in the vicinity of the junction. (a) $d_3/d_1 = 1.0$, flow condition 2; (b) $d_3/d_1 = 0.5$, flow condition 3.

of the side branch bubble sizes are generally comparable with those of the main outlet, whilst quite large voids with average detected chordal lengths of up to 50 mm are found in the upper half. Clearly these can not be approximately regarded as spherical voids, and for this reason the results are shown as detected chordal lengths rather than interpreting these in terms of bubble diameters on the basis of the assumptions of spherical shape (see Herringe & Davis 1976). The results thus show the combined effects of turbulent losses at the junction, acting to substantially reduce bubble size in flow regions where the gas and liquid are well-mixed, and of stratification in the side branch, giving rise to the occurrence of quite large gas voids in the upper half of the branch flow moving at a higher velocity than the remainder of the flow.

Observation of intermittent flow fluctuations were made by passing the void probe two-state signal through a low-pass filtering average circuit, as described by Fungtamasan & Davis (1984). This allowed resolution of the relatively slow fluctuations of local void fraction which occurred at frequencies of ~ 20 Hz, these being much slower than the passage of individual voids which occurred at frequencies of ~ 1000 Hz typically. In general, the voidage fluctuations in the inlet and side branch were random in nature with a broad distribution of fluctuation energy over the range to ~ 20 Hz, whilst there was a distinct tendency for fluctuations at 5–6 Hz to occur in the main outlet flow when the average velocity there was above 3.5 m/s. At lower velocities the main outlet voidage fluctuations were similar to those in the inlet and broadband in nature with no particular dominant frequency component. The r.m.s. amplitude of these voidage fluctuations was on average 0.35 of the mean local voidage in the inlet flow, with a relatively steadier flow in the branch having an r.m.s. voidage fluctuation of 0.20 of the mean local voidage. In the main outlet conditions were significantly less steady, with r.m.s. voidage fluctuations increasing to about 0.69 of the mean local voidage. However, in general, these levels of relatively slow fluctuation of local voidage were not sufficient to give rise to the formation of distinctive slugs of gas, and the flows thus lie in the churn or bubbly flow regions and exhibit a significant level of unsteadiness at low frequency in the local mixture voidage.

It was possible to measure the cross-correlation between the low frequency voidage fluctuations at the inlet and either of the two outlets, and thus to determine the time for low-frequency voidage pulsations to propagate through the junction. Maximum values of the correlation coefficient occurred at times corresponding to the transport time through the junction and had values of about 0.2, indicating that the junction had significantly distorted the patterns of void fraction variations

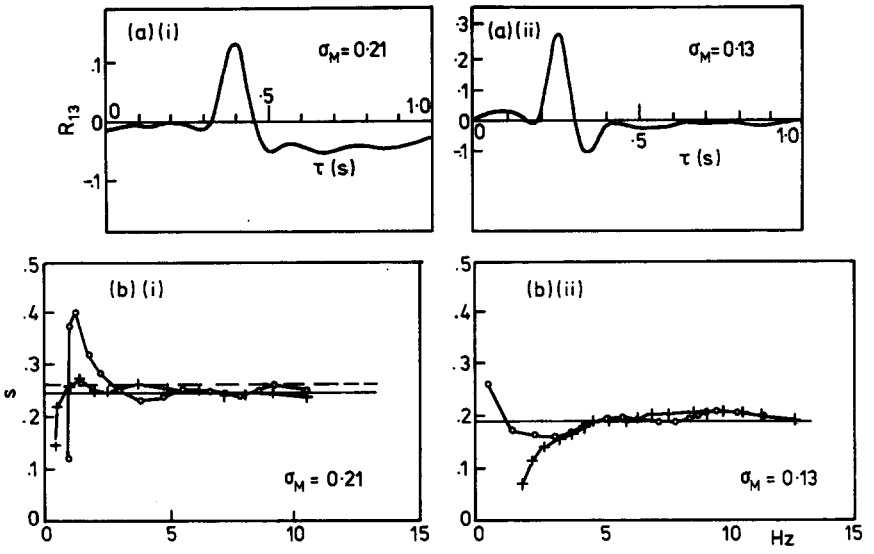

Figure 7. Variation of time for the propagation of voidage fluctuations through the junction with the frequency of fluctuation. (a) Cross-correlation function between sections 1 and 3. (b) Transport time spectrum between sections 1 and 3. (i) $d_3/d_1 = 1.0$; (ii) $d_3/d_1 = 0.5$ (flow condition 3). ○, between sections 1 and 2; +, between sections 1 and 3.

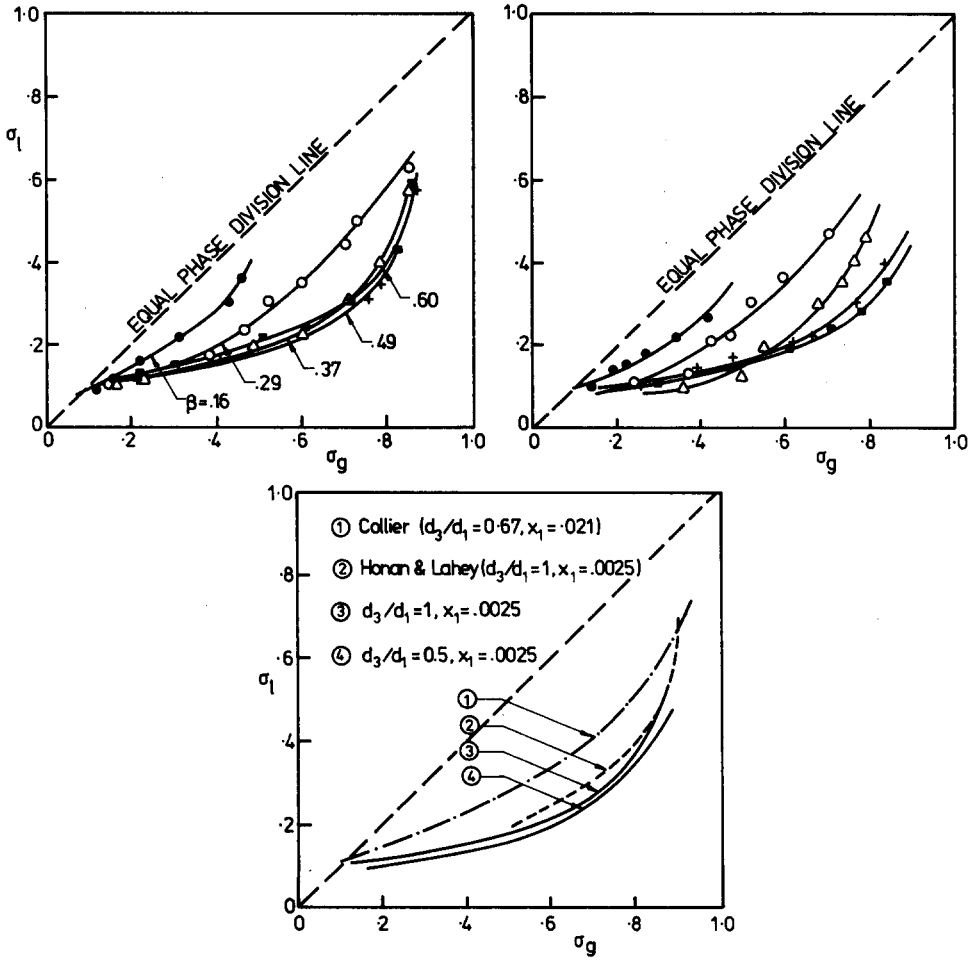

Figure 8. Subdivision of phases between the branch and main outlet pipes. (a) $d_3/d_1 = 1.0$. (b) $d_3/d_1 = 0.5$. (c) ① Collier (1976) ($d_3/d_1 = 0.67$, quality = 0.021); ② Honan & Lahey (1978) ($d_3/d_1 = 1$, quality = 0.0025); ③ present data ($d_3/d_1 = 1$, quality = 0.0025); ④ present data ($d_3/d_1 = 0.5$, quality = 0.0025). Flow conditions: ●, 1; ○, 2; △, 3; +, 4; ■, 5.

as they moved through the junction. It was found that, on average, the voidage fluctuations passed through the junction at between 1.05 and 1.58 times the superficial average mixture velocity (based on volumetric flow rates). The transport time was relatively constant over all frequencies, as illustrated in figure 7 which shows the dependence of transport time on frequency, obtained by Fourier transformation of the cross-correlation function into the phase spectrum and by division by frequency to obtain the transport time. In general, it thus appears that the voidage fluctuations move more rapidly than the average mixture velocity, a result consistent with the observation of velocity ratios (S, figure 5) also in the range between 1.0 and 1.5.

(iii) Subdivision of the flow by the junction

The subdivision of the two phases by the junctions was measured directly from the overall mass flow measurements in the inlet and branch outlets. For a given inlet flow condition adjustments were made to the regulating valves on the branch and main outlets so that differing branch take-off flows were achieved. The results of these tests are shown in figure 8, from which it can be seen that in all cases a proportionately higher fraction of the gas flow is diverted to the branch. This effect increases relatively as the branch take-off is increased, and also with an increase in the mixture inlet void fraction. These results are generally consistent with the observations of Collier (1976) at a much higher gas content and of Honan & Lahey (1978), and also with the recent work of Hwang *et al.* (1988) who also reported data for subdivision of 40° angle junctions of equal branch and main pipe areas. It appears that since the inlet flow has an appreciably higher gas content near the flow centreline, the performance of the junction is dominated by the separation of phases induced by the pressure gradients in the junction itself and by the substantially greater inertia of the liquid phase, which makes it very much less responsive to the transverse pressure gradients which must exist towards the side branch. These results are in general conformity with those of Hoang & Davis (1984), who found that similar inlet flows to a 180° bend induced considerable separation of phases within the bend, and it thus appears that the gas and liquid phases are relatively weakly coupled. The occurrence of velocity ratios in the range up to 1.5 also reflects this generally weak coupling of the phases, and it would appear that the restriction of velocity ratios to even this value is a consequence of the mixing of phases over relatively long distances within one-dimensional pipe flows without the much more rapid changes of flow momentum that are induced at pipe components such as branch junctions and bends. As has been seen, this process is probably influenced significantly by the concentration of gas into bubble clouds along the flow axis. However, the branch flow, although stratified, is relatively much better homogenized along the flow direction than is the main outlet flow, reflecting the strong induced mixing effects which would be associated with the extraction of relatively high proportions of the gas phase from the central region of the main pipe flow through the outer region of much lower gas content.

4. PRESSURE LOSS THROUGH THE JUNCTION

Detailed observations were made of the pressure distributions around the circumference of the inlet and outlet pipes in the immediate vicinity of the junction, and some examples are shown in figure 9. The pressures on the main pipe walls are higher on the side opposite to the junction, reflecting the requirement to provide a force in that direction to sustain the side branch momentum flux. In the side branch the pressure is higher on the side furthest from the inlet pipe, thus providing a force component in a direction opposite to the inlet flow to reduce the momentum flux in the inlet flow direction. The magnitude of these pressure differentials is in the range extending to approx. 0.5 m of water head. This corresponds quite closely to the dynamic pressure rise of the inlet flow, as would be expected. The present results are not sufficiently detailed to form a basis for calculation of the force coefficients k_x and k_y from integration of the wall pressure distributions, but it can be seen that k_x and k_y, [7] and [8], would be expected from these limited observations to be of a magnitude in the range of approx. 0.5.

Streamwise distributions of wall static pressures are shown in figure 10. The results show quite clearly the development of frictional pipe flow in the three pipes away from the junction where the pressures reduce steadily in the flow direction. In the main inlet and outlet pipes these frictional

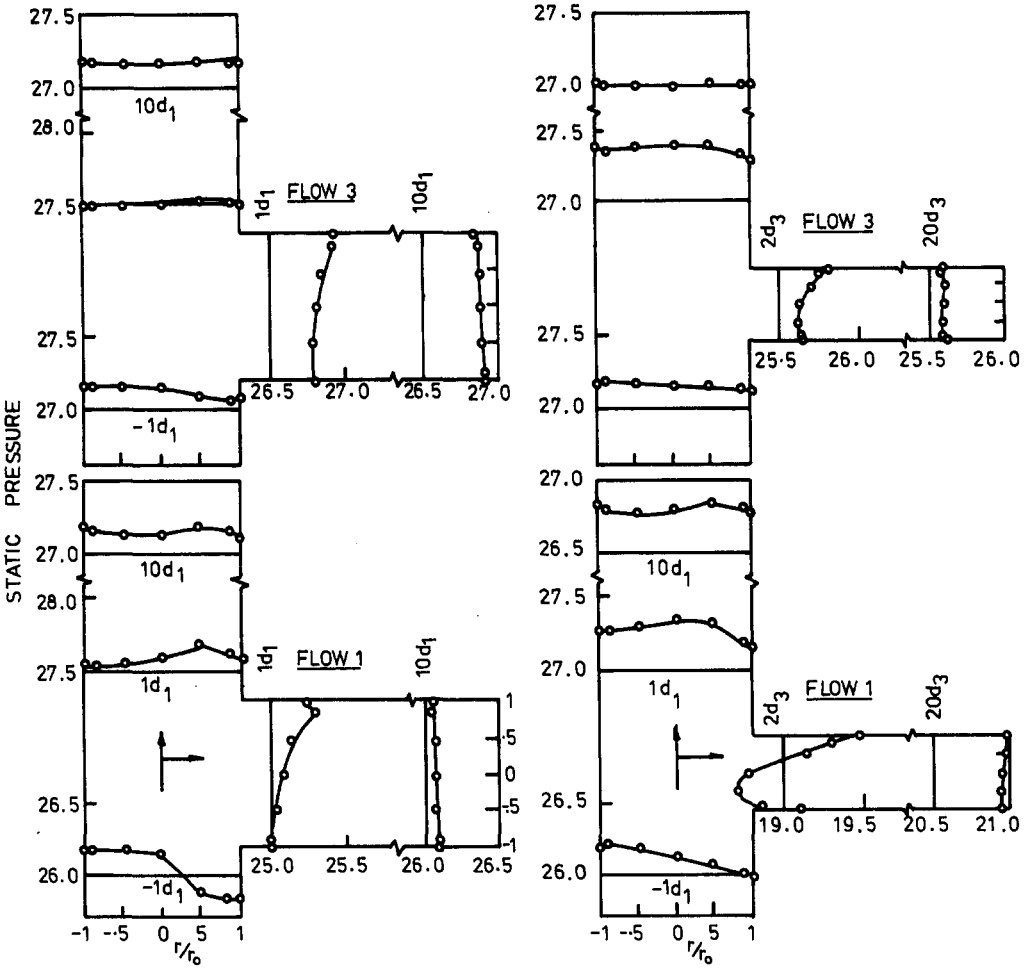

Figure 9. Wall pressure distributions in the vicinity of the junction. [Figures denote static pressures at the wall (metres of water), gauge positions indicate the distance from the junction of observations.]

profiles are maintained quite close to the junction, whilst in the branch pipe the transitional process for development of frictional pipe flow appears to extend for a greater distance from the junction. From these observations it was possible to define a distinct settling length required in the side branch in terms of the position where the steady frictional pressure drop commenced. It can be seen from figure 11 that the normalized transition length was larger in the case of the smaller tube when the side branch diameter was used as a reference. Since there is approximately a 1.5 : 1 difference in these normalized settling lengths with $d_3/d_1 = 0.5$ and 1.0, it follows that the settling lengths were physically quite similar for the two test junctions. The results show a clear trend for the transition length to reduce as the mixture gas volume flow fraction increased, and for the transition length to increase with mixture Reynolds number (calculated here on the basis of mixture average density and velocity, the pipe diameter and the liquid velocity). As a further check on these observations, the slopes of the frictional pipe flow pressure drop lines for the inlet and outlet pipes and the mixture mean flow conditions in each pipe were used to calculate the friction factor for each pipe using the compressible gas–liquid flow relations of Davis (1974). The results are shown in figure 12, and indicate only approximate agreement with the experimental correlations of Davis (1974). The rather higher values observed in the inlet pipe here may be due to the fact that the present data commence at the mixer outlet and that the flow is not fully developed over at least the first part of the inlet pipe length. The main outlet results show quite close consistency with the results of Davis (1974), whilst the rather lower friction factors found in the branch pipe may be due again to the absence of a long settling length to establish a fully developed (in this case stratified) pipe flow.

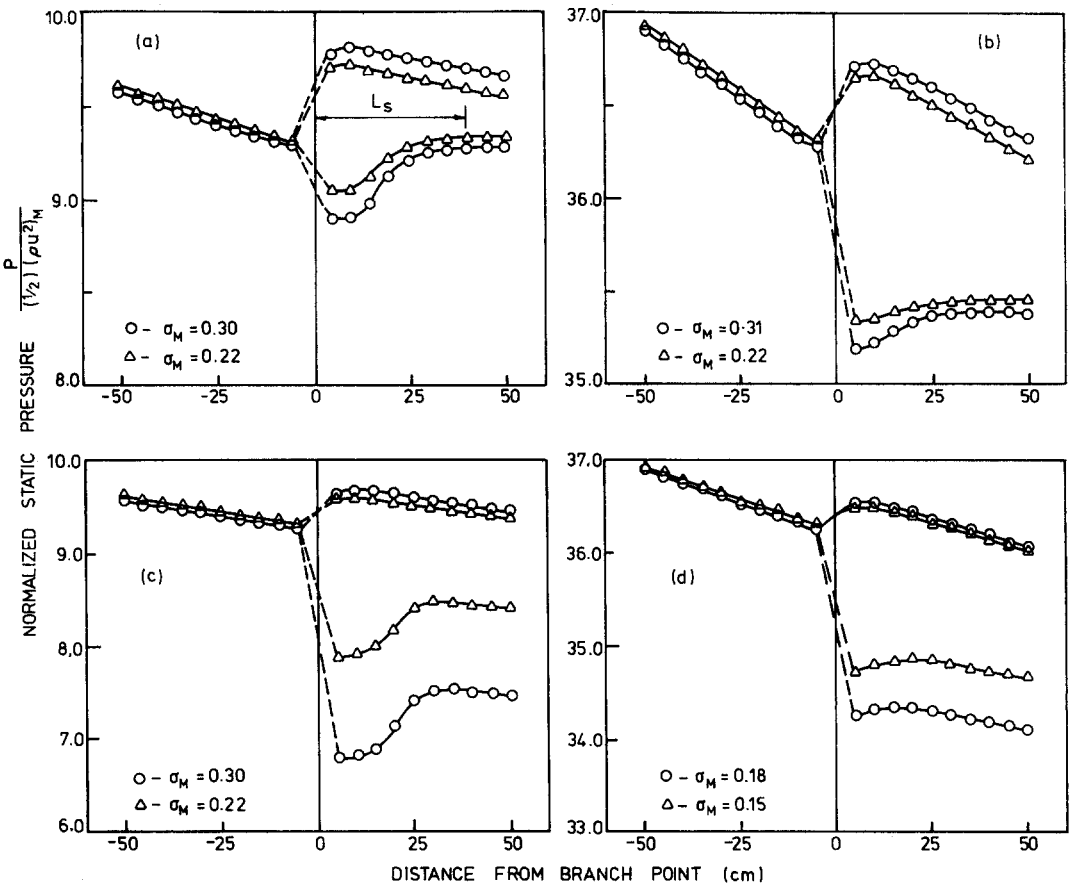

Figure 10. Streamwise distributions of wall static pressure. (a) $d_3/d_1 = 1$, flow condition 1; (b) $d_3/d_1 = 1.0$, flow condition 3; (c) $d_3/d_1 = 0.5$, flow condition 1; (d) $d_3/d_1 = 0.5$, flow condition 3. (Flow left to right: main inlet data to the left of the junction point; main outlet data on the upper curves to the right; and branch outlet data on the lower curves to the right.)

Having thus confirmed that the steady pressure drop sections of the observed axial pressure profiles do correspond to the condition of frictional pipe flow, and also having established that a certain transition distance exists where the junction influences the flow, it was possible to extrapolate the frictional pressure drop lines back to the junction point so as to define values of $(p_3 - p_1)$ and $(p_2 - p_1)$, as illustrated in figure 10. The extrapolation was based on the section of the axial pressure distributions showing a steady frictional pressure gradient. The dotted lines in figure 10 merely serve to link corresponding sections of data, and are not intended to indicate pressures at the junction. The observed pressure changes across the junction are shown in

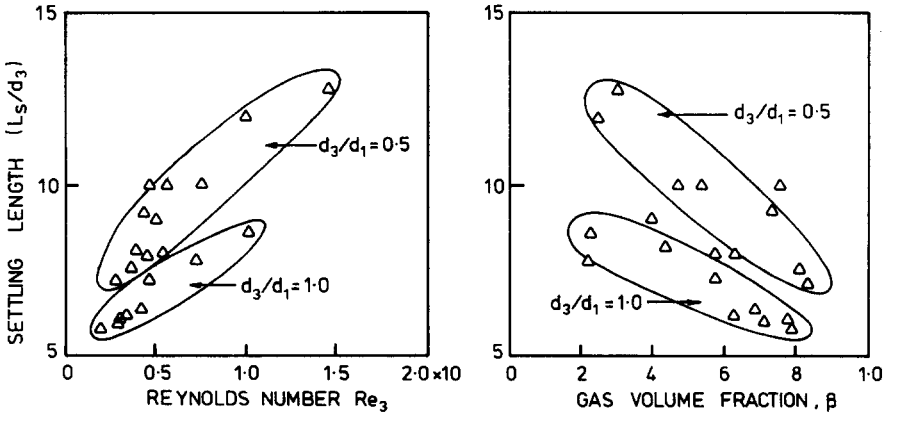

Figure 11. Length required for the re-establishment of developed frictional pipe flow in the branch.

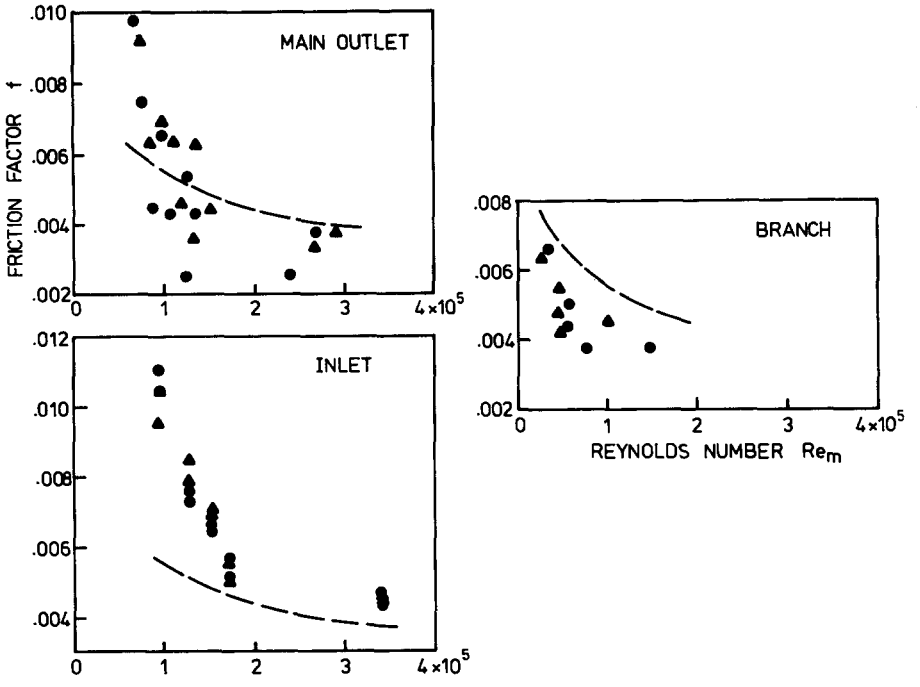

Figure 12. Friction factors for frictional pipe flow in the branch and main pipes. — —, Davis (1974), long pipe correlation; ●, $d_3/d_2 = 1$; ▲, $d_3/d_2 = 0.5$.

figure 13, and are seen to be in general conformity with the predicted dependence upon take-off ratio shown in figure 2. These results were then combined with the velocity ratios (S) and flow distribution parameters (C_m, C_e) determined from the void probe observations, described in section 3, and [12] and [13] were used to determine the junction force coefficients k_x and k_y. This process thus allows for compressibility of the gas–liquid mixture flow and also for the distribution of voidage and velocity actually existing in the flow in the calculation of k_x and k_y. As will be seen, presentation of these results in terms of the force coefficients k_x and k_y allows a direct comparison to be made with single-phase flow data and, for this reason, force coefficient results rather than the actual net junction forces (F_x and F_y) are presented here. The results for all five test flows with the two test junctions are shown in figure 14 for overall mixture take-off fractions in the range 0.1–0.35. The streamwise force coefficient k_x was found to lie in the range 0.5–0.7, with a tendency for this to reduce as the mixture void fraction increased to about 0.5, and then to increase again. This behaviour is somewhat similar to that observed for the subdivision of the flow, which gave

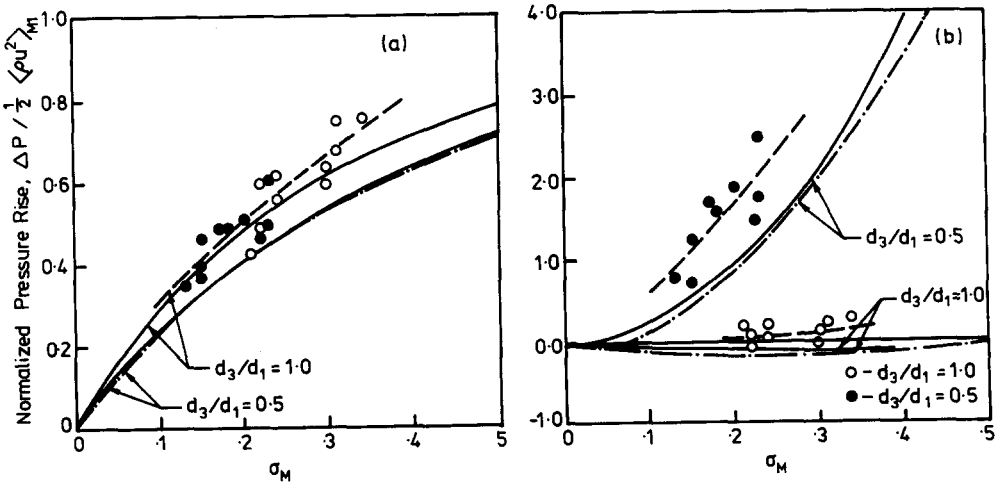

Figure 13. Normalized pressure changes across the junction. (a) Inlet to the main outlet. (b) Inlet to the branch. ——, Miller (1978); — · —, McNown (1954).

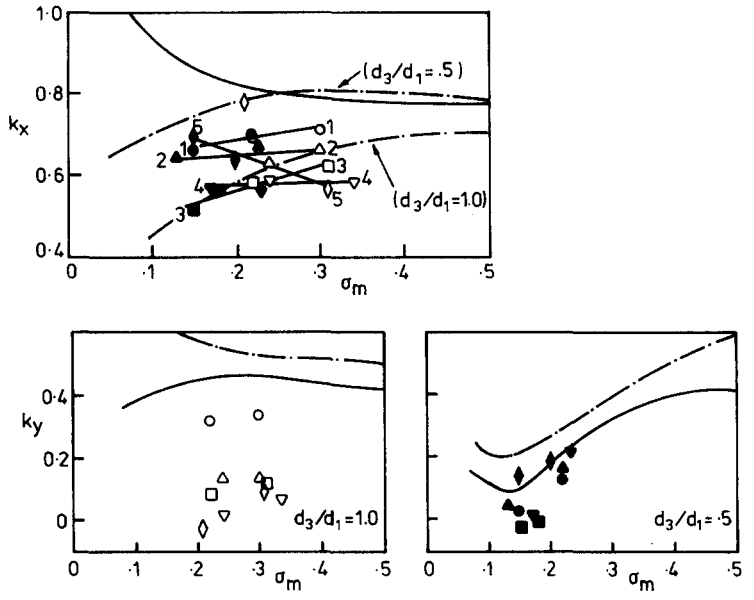

Figure 14. Net force coefficients for the junction in the main (k_x) and branch (k_y) directions. ——, Miller (1978); — · —, McNown (1954). Open symbols, $d_3/d_1 = 1.0$; closed symbols, $d_3/d_1 = 0.5$. The flow conditions are denoted by numbers.

an increasing branch relative gas flow up to a void fraction of about 0.5 with a tendency for the relative gas flow to reduce at higher void fractions (figure 8). Whilst the present results clearly lie close to the values of k_x observed by McNown (1954) and Miller (1971) for single-phase flows, the indication of an increase in k_x as the branch size is reduced was not as clear in the present tests. This may, in part, be due to the relatively strong obscuring effect of the gas content in these two-phase flow tests which reduces k_x with increasing gas content, although it can be seen in figure 14 that there is an indication of a value of k_x nearer to the McNown line for $d_3/d_1 = 0.5$ in the two-phase tests for that branch size. The observed values of the transverse force coefficient k_y are seen to lie quite close to the results of Miller (1971) for the smaller sized branch [figure 14], whereas in the case of the larger sized branch ($d_3/d_1 = 1.0$) the results are considerably smaller than those of Miller (1978) and McNown (1954). In considering these results it needs to be borne in mind that the definition of the coefficient k_y, [8], adopted here follows the approach adopted by these previous authors for single-phase flow. As has been seen, the gas content of the side branch flow is proportionately much higher than for the inlet flow, and thus the use of the inlet mixture flow density in the definition of the transverse force coefficient is probably not entirely appropriate since the transverse forces are more likely to scale with the density and velocity in the side branch.

The loss of stagnation pressure which the flow experiences in passing from the inlet to each outlet flow can be determined if the stagnation pressure in each flow is related to the observed local conditions. The process of flow stagnation is governed by the one-dimensional momentum equation in the flow direction x, this being (see Davis 1980), in terms of area-averaged quantities,

$$\frac{dp}{dx} + \epsilon\rho_G u_G \frac{du_G}{dx} + (1-\epsilon)\rho_L u_L \frac{du_L}{dx} = 0. \qquad [24]$$

Introduction of the equations of state given in section 2 and integration then leads to the following equation for the stagnation pressure p_s in terms of the local pressure p and under the limitations of the definition of an average velocity ratio S as discussed above:

$$\langle(1-\epsilon)\rangle\left[\left(\frac{p_s}{p}\right)-1\right] + \langle\epsilon\rangle\log_e\left(\frac{p_s}{p}\right) = \frac{D}{2}. \qquad [25]$$

We can then define stagnation pressure loss coefficients for the main and branch outlet flows as

$$K_{12} = \frac{\frac{p_{s1}}{p_1} - \frac{p_{s2}}{p_1}}{\frac{D_1}{2}} \qquad [26]$$

and

$$K_{13} = \frac{\frac{p_{s1}}{p_1} - \frac{p_{s3}}{p_1}}{\frac{D_1}{2}}. \qquad [27]$$

The results thus obtained for this pressure loss coefficients are shown in figure 15, and once again these are compared with the single-phase results of Miller (1978) and McNown (1954). It can be seen that negative pressure loss coefficients are obtained for K_{12}, and that the two-phase results here lie between the results of Miller and McNown who also observed negative values for K_{12}. The result was attributed by McNown to the fact that the branch flow under single-phase conditions draws on the outer region of the inlet flow, which has a lower than average kinetic energy due to the distribution of velocity in the inlet flow. It appears that the same phenomenon occurs under the two-phase conditions observed here. It is possible that the effect observed in single-phase flows is compounded under two-phase conditions by the division of a higher proportion of the gas phase with lower kinetic energy to the branch, allowing a higher proportion of liquid to remain in the main outlet flow which thereby retains above the average kinetic energy of the inlet flow. It can be seen from figure 15 that substantially higher pressure loss coefficients to the branch occur under two-phase conditions, although there is a similar increase in the branch loss coefficient with reducing side branch diameter to that observed by Miller and McNown for single-phase flow. Once again this is attributable to the division of a relatively high proportion of the gas phase to the branch under two-phase flow conditions. In general terms, it appears that the two-phase flow exhibits a similar behaviour to the single-phase flow, but that this is modified by the proportionate division of the two phases to the main and branch outlets.

5. CONCLUSIONS

If account is taken of the internal structure and compressibility of the gas–liquid mixture flow in terms of the velocity ratio and the momentum and kinetic energy distribution coefficients, as discussed, it is found that the two-phase flow at a branch junction behaves in a generally similar

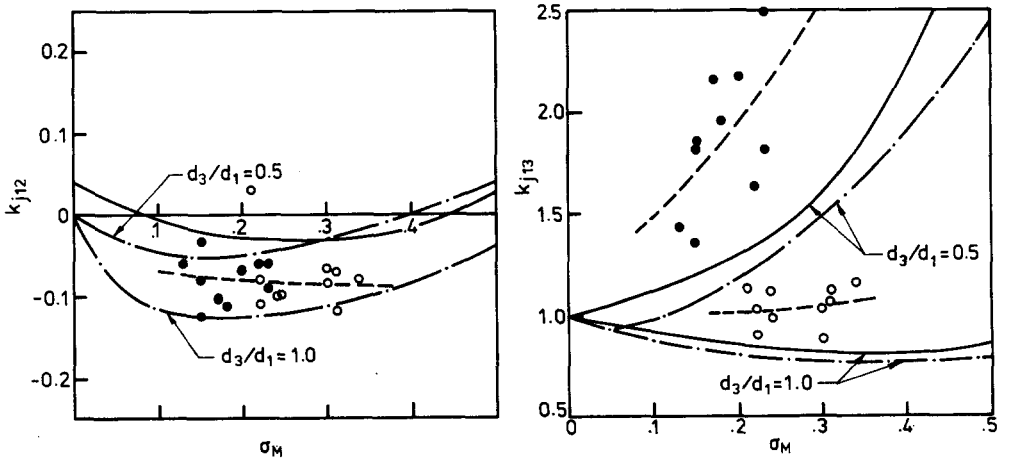

Figure 15. Pressure loss coefficients for flow through the junction. ——, Miller (1978); – – –, McNown (1954); — · —, present data. ○, $d_3/d_1 = 1.0$; ●, $d_3/d_1 = 0.5$.

manner to single-phase flow. Values for the junction force and pressure loss coefficients have broadly the same values as in single-phase fow, except that the unequal subdivision of phases to main and branch flows rise to significantly smaller values of the transverse force coefficient and to larger values of the branch pressure loss coefficient for the two-phase flow case. The characteristic diversion of higher proportions of the gas phase to the side branch was found to increase with inlet flow void fraction and also with increases in the overall proportion of flow drawn off into the branch.

Observations of the flow structure near the junction showed the side branch flow to be stratified, but that the flow in the branch was somewhat smoother than that in the main pipe in terms of the magnitude of the unsteadiness of void fraction at points in the flow. The main outlet flow tended to have a velocity maximum on the side where the branch was located, and also exhibited a strong tendency to develop stronger unsteadiness of local void fraction with a Stronhal number of approx. 0.1, indicating the presence of intermittent pulsations of void fraction extending over a length of approx. 10 pipe diameters. Fungtamasan & Davis (1984) also found similar pulsations to be present in a straight vertical pipe under similar flow conditions, and it appears that the development of these regular pulsations under some conditions of flow has been accentuated by the extraction of flow at the junction. These pulsations of void fraction were found to propagate through the junction at a velocity in excess of the mixture velocity.

The length required for re-establishment of steady pipe flow in the side branch was found to increase with the Reynolds number of the branch flow, and to decrease with the average void fraction in the branch flow.

REFERENCES

ACRIVOS, A., BABCOCK, B. D. & PIGFORD, R. L. 1959 Flow distribution in manifolds. *Chem. Engng Sci.* **1,** 112–124.

AZZOPARDI, B. J. & WHALLEY, P. B. 1982 The effect of flow patterns on two phase flow in a T-junction. *Int. J. Multiphase Flow* **8,** 491–507.

BAJURA, R. A. 1971 A model for flow distribution in manifolds. *Trans. ASME Jl Engng Power* **93,** 7–12.

BENSON, R. S. & WOOLATT, D. 1966 Compressible flow loss coefficients at bends and T-junctions. *Engineer* 28 Jan.

COLLIER, J. G. 1976 Single-phase and two-phase flow behaviour in primary circuit components. Lecture presented at the *NATO Advanced Study, Inst. on Two-phase Flows and Heat Transfer*, Istanbul, Turkey.

CROW, D. A. & WHARTON, R. A. 1968 A review of literature on the division and combination of flow in closed conduits. BHRA Report TN937.

DAVIS, M. R. 1974 The determination of wall friction for vertical and horizontal two-phase flow. *Trans. ASME Jl Fluids Engng* **96,** 173–179.

DAVIS, M. R. 1980 Response of small Pitot tubes in gas–liquid flows. *Int. J. Multiphase Flow* **6,** 369–373.

ENGER, M. L. & LEVY, M. I. 1929 Pressures in manifolds. *J. Am. Wat. Wks Ass.* **21,** 659–667.

FOUDA, A. E. & RHODES, E. 1972 Two-phase annular flow stream division. *Trans. Instn chem. Engrs* **50,** 353–363.

FOUDA, A. E. & RHODES, E. 1974 Two-phase annular flow stream division in a simple tee. *Trans. Instn chem. Engrs* **52,** 354–360.

FUNGTAMASAN, B. & DAVIS, M. R. 1984 Large scale structures in gas–liquid mixture flows. *Int. J. Multiphase Flow* **10,** 663–676.

GARDEL, A. 1957 Pressure drops in flow through T-shaped pipe fittings. *Bull. tech. Suisse romande* **Apr./May,** 123–130 (in French).

GREENE, J. L. 1967 Symmetrical piping arrangement solves two-phase Refin. *Hydrocarbon Process.* **46,** 141–143.

HERRINGE, R. A. & DAVIS, M. R. 1974 Detection of instantaneous phase changes in gas–liquid mixture flow. *J. Phys. scient. Instrum.* **E7,** 807–812.

HERRINGE, R. A. & DAVIS, M. R. 1976 Structural development of gas–liquid mixture flows. *J. Fluid Mech.* **73,** 97–123.

HOANG, K. & DAVIS, M. R. 1984 Flow structure and pressure loss for two phase flow in return bends. *Trans. ASME Jl Fluids Engng* **106,** 30–37.

HONAN, T. J. & LAHEY, R. T. 1978 The measurement of phase separation in wyes and tees. Report, RPI Research Project No. 5-24510.

HONG, K. C. 1978 Two-phase flow splitting at a pipe tee. *JPT* **30,** 290–296.

HWANG, S. T., SOLIMAN, H. M. & LAHEY, R. T. JR 1988 Phase separation in dividing two phase flows. *Int. J. Heat Mass Transfer* **14,** 439–458.

ITO, H. & IMAI, K. 1973 Energy losses at 90° pipe junction. *Proc. ASCE Jl hydraul. Div.* **99,** 1353–1368.

JAMISON, D. K. & VILLEMONTE, J. R. 1971 Junction losses in laminar and transitional flows. *Proc. ASCE Jl hydraul. Div* **97,** 1045–1063.

KATZ, S. 1967 Mechanical potential drops at a fluid branch. *Trans. ASME Jl bas. Engng* 732–736.

MADDEN, J. M. & ST PIERRE, C. C. 1970 Two-phase air–water flow in a slot-type distributor. *Proc. Instn mech. Engrs* **3c,** 175–184.

MCNOWN, J. S. 1954 Mechanics of manifold flow. *Trans. ASCE* **119,** 1103–1142.

MCNOWN, J. S. & HSU, Y. E. 1951 Application of conformal mapping to divided flow. In *Proc. 1st Midwestern Conference on Fluid Dynamics, Univ. of Illinois, 1950.* Edwards, Ann Arbor, Mich.

MILLER, D. S. 1971 *Internal Flow: a Guide to Losses in Pipe and Duct Systems.* BHRA, Cranfield, Beds.

MILLER, D. S. 1978 *Internal Flow Systems.* BHRA, Cranfield, Beds.

ORANJE, L. 1973 Condensate behaviour in gas pipelines is predictable. *Oil Gas J.* 2 July.

PETERMANN, F. 1929 Loss in oblique-angled pipe branches. *Mitt. hydraul. Inst. Münch.* **3.**

TAITEL, Y., BORNEA, D. & DUKLER, A. E. 1980 Modelling flow pattern transition for steady upward gas–liquid flow in vertical tubes. *AIChE Jl* **22,** 345–354.

TSUYAMA, M. & TAGA, M. 1959 On the flow of the air–water mixture in the branch pipe. *Bull. JSME* **2,** 151–156.

VOGEL, G. 1926/28 Investigation of the loss in right-angled pipe branches. *Mitt. hydraul. Inst. Münch.* **1,** 75–90 (1926); **2,** 61–63 (1928). In German. [Translation by VOETSCH, C., U.S. Dept of the Interior, Denver, Colo., Technical Memo 299 (1932).]

WILLIAMSON, J. V. & RHONE, T. J. 1973 Dividing flow in branches and wyes. *Proc. ASCE Jl hydraul. Div.* **99,** 747–769.

YADIGAROGLU, G. & LAHEY, R. T. JR 1976 On the various forms of the conservation equations in two phase flow. *Int. J. Multiphase Flow* **2,** 477–494.

ZEISSER, M. H. 1963 Summary report of single tube branch, multitube branch water flow test conducted by the University of Connecticut. Pratt and Whitney Aircraft Div., Report No. PWAC-231, USAEC Contract AT (1101)-229.

ZUBER, N. & FINDLAY, J. A. 1965 Average volumetric concentration in two-phase flow systems. *Trans. ASME Jl Heat Transfer* **87,** 453–468.